J. Fluid Mech. (1995), *vol.* 283, *pp.* 287–305

The effect of deformable porous surface layers on the motion of a sphere in a narrow cylindrical tube

By WEN WANG AND KIM H. PARKER

Physiological Flow Studies Group, Centre For Biological and Medical Systems, Imperial College of Science, Technology and Medicine, London SW7 2BY, UK

(Received 1 November 1993 and in revised form 12 August 1994)

The hydrodynamic influence of deformable porous surface layers on the motion of a rigid sphere falling in a narrow cylindrical tube filled with a stationary Newtonian fluid is studied using lubrication theory. The porous layers on both the surface of the tube and the sphere are modelled as binary mixtures of solid and liquid components. The sphere is placed at an arbitrary position in the tube and is free to rotate. Effects of the clearance between the sphere and the tube, the eccentricity of the position of the sphere and the properties of the surface layers on the velocity and rotation of the sphere are studied. It is found that, when the lengthscale on which the velocity varies within the porous layer is much smaller than the clearance, the effects of the porous layer can be represented by an equivalent slip boundary condition, the slip velocity at the boundary being proportional to the local shear rate. The slip velocities have a strong influence on the motion of the sphere when the clearance is small. For a given clearance and slip parameters, both the falling and rotation velocities of the sphere increase with the sphere eccentricity. The shear stresses on the surfaces of both the tube and the sphere are greatly reduced when slip boundary conditions are applied, as is the pressure gradient in the region between the sphere and the tube wall. This work could have some relevance to the creeping motion of blood cells in the microcirculation where the glycocalyx, a polysaccharide-rich layer, covers the external surfaces of both endothelial and red blood cells.

1. Introduction

This study is motivated by the problem of the motion of blood cells in a small capillary. Capillaries are the smallest blood vessels in the body, about 6–12 μm in diameter. They are lined with a layer of endothelial cells, through which the plasma and blood cells flow. The plasma itself is known to behave as a Newtonian viscous fluid although it contains several types of protein molecules in suspension (Cokelet *et al.* 1963; Merrill *et al.* 1965). There is increasing interest in the effects of blood flow on vascular endothelial cells because of the possible influence of flow on vascular biology and pathobiology (Nerem & Girard 1990; Fung & Liu 1993). Many properties of endothelial cells in culture depend upon the fluid dynamical conditions in the culture medium. The mechanisms underlying these effects are unclear but it seems plausible that cell–fluid interactions are mediated or at least influenced by the glycocalyx. The glycocalyx is a broad term for all polysaccharide-containing structures on the external surface of cells. Both red blood cells and endothelial cells possess glycocalyx. It contains glycoproteins, which are complex branched flexible highly charged molecules, and also plasma proteins, such as albumin and fibrinogen. Its thickness is about 50–80 nm in arteries (Haldenby *et al.* 1994) and is estimated to be up to 1 μm in

capillaries (Silberberg 1991). It is difficult, however, to determine its composition quantitatively. Arguments based on the behaviour of similar molecules in tissue or model systems suggest that it has the physical properties of a viscoelastic gel (Curry 1984). Being the outer barrier between the environment and the cell, the surface component may play an important role in controlling the immediate external cell environment and thereby influence many transmembrane transport and transduction processes. Its influence on vessel wall shear stress may also be linked to the development of atherosclerosis in arteries (Caro 1982).

In this paper, we consider a simplified model which will have some relevance to the motion of a blood cell in a capillary: a sphere falling in a cylindrical tube with thin uncharged deformable porous layers on the surfaces of both the sphere and the tube. In the microcirculation, the elastic properties of red blood cell membranes allows them to deform when exposed to shear stresses (Secomb *et al.* 1986) and there are generally a number of red blood cells in a single capillary, although Wang & Skalak (1969), in a model study of a train of spheres in a narrow capillary, conclude that the spheres behave independently when they are more than one diameter apart. Also, blood cells are driven by a pressure difference, whereas in the model we consider the simpler condition of the motion of a sphere under gravity which will allow us to focus on the hydrodynamic influence of the glycocalyx layer. The radius of the tube is taken to be only slightly larger than that of the sphere, so that the clearance between the sphere and the tube is small compared with the radius of the sphere. The Reynolds number of the flow is much smaller than 1. Lubication theory is applicable in a region around the equator of the sphere. The pressure drop across the lubrication zone is linearly related to the weight of the sphere.

Brenner & Happel (1958) studied the problem of the motion of a sphere in a tube using a reflection method, in which the sphere is constrained not to rotate and the solution is valid when the radius of the sphere is much smaller than that of the tube. Bohlin (1960) gave an approximate solution for a sphere moving on the axis of a tube, using an extension of the reflection method. The motion of a sphere taking an eccentric position in a tube was studied using lubrication theory (Christopherson & Dowson 1959). There are, however, two assumptions in their work which are not warranted *a priori*: (i) they assumed that the stable position of the sphere could be determined by the minimum energy dissipation; (ii) they assumed that lubrication theory, which should be valid only inside the lubrication region around the line of minimum clearance between the sphere and the tube, was applicable throughout the gap. Bungay & Brenner (1973) used a singular perturbation technique to study this problem in the absence of surface layers and showed that the lubrication approximations are the leading-order terms of a perturbation expansion. Chester (1984) studied the motion of a sphere in a slightly tilted tube where the eccentricity can be calculated by a force balance between the components of gravity and the net force due to pressure in the direction normal to the tube axis. Numerical methods have also been used by a number of researchers to study the motion of a sphere in a tube filled with Newtonian or non-Newtonian fluid; however, they were concerned mainly with non-Newtonian effects and the fixed sphere at the centre of the tube. The interesting problem of the rotation of a sphere is not addressed.

In this paper, lubrication theory is used in a region around the equator of the sphere and the influence of deformable porous layers on the motion of the sphere, the flow field and the wall shear stress are investigated. Similar notation to that of Christopherson & Dowson (1959) is used and comparison is made with Bohlin's (1960) approximate solution when the sphere is at the centre of the tube and no-slip boundary

conditions are applied. Comparison is also made with Christopherson & Dowson's result when the sphere has an eccentric position, the clearance is small and no-slip boundary conditions are applied.

2. Deformable porous layer

The theory of mixtures has been used to model arterial wall permeability (Kenyon 1979), articular cartilage (Lai, Hou & Mow 1991) and skin (Lanir *et al.* 1990). Most analyses have considered only one-dimensional or purely radial compression. Recent papers have considered the deformation of a porous surface layer in a shear flow (Hou *et al.* 1989; Barry, Parker & Aldis 1991).

2.1. *Governing equations in the porous medium*

The theory of mixtures used here is based on the work of Kenyon and Bowen (Kenyon 1976; Bowen 1980). The porous medium is modelled as a binary mixture of solid and fluid phases; each point inside the porous medium is considered to be occupied by both solid and fluid phases simultaneously. It is assumed that there are no body forces in the porous medium. The solid phase is incompressible and has a homogenous isotropic structure and linear elasticity. The liquid phase is an incompressible Newtonian fluid with its volume fraction represented by φ so that the volume fraction of the solid phase is $1-\varphi$. The volume-averaged densities of the phases are represented by ρ_f and ρ_s. The mass conservation equations derived by Mow *et al.* (1985) give, at steady state

$$\nabla\cdot\boldsymbol{q} = 0, \tag{2.1}$$

$$\nabla\cdot\dot{\boldsymbol{s}} = 0, \tag{2.2}$$

where $\boldsymbol{q}$ stands for the fluid velocity inside the porous material, $\boldsymbol{s}$ is the solid displacement vector and $\dot{\boldsymbol{s}}$ is the solid velocity. Assuming infinitesimal solid deformation in the porous medium, φ can be taken as a constant, and for sufficiently small Reynolds number, the momentum equations for the two phases are

$$\nabla\cdot\boldsymbol{T}^f + k(\dot{\boldsymbol{s}}-\boldsymbol{q}) = 0, \tag{2.3}$$

$$\nabla\cdot\boldsymbol{T}^s - k(\dot{\boldsymbol{s}}-\boldsymbol{q}) = 0, \tag{2.4}$$

where $\boldsymbol{T}^f$ and $\boldsymbol{T}^s$ are the stress tensors for fluid and solid phases respectively, $k = \mu_f/K$ is the drag coefficient with μ_f the fluid viscosity and K the flow permeability of the porous material. The last term in the momentum equation is an internal interaction force between the solid and fluid phases. The stress tensor can be expressed as

$$\boldsymbol{T}^f = -\varphi p\boldsymbol{I} + 2\mu_a\boldsymbol{\varepsilon}, \tag{2.5}$$

$$\boldsymbol{T}^s = -(1-\varphi)p\boldsymbol{I} + \lambda\nabla\cdot\boldsymbol{s}\boldsymbol{I} + 2\mu\boldsymbol{e}, \tag{2.6}$$

where p is the volume-averaged pressure, $\boldsymbol{I}$ is the identity matrix, $\boldsymbol{\varepsilon} = \frac{1}{2}(\nabla\boldsymbol{q} + \nabla\boldsymbol{q}^T)$ is the rate-of-strain tensor for the fluid component, $\boldsymbol{e} = \frac{1}{2}(\nabla\boldsymbol{s} + \nabla\boldsymbol{s}^T)$ is the solid deformation tensor, μ and λ are the Lamé coefficients and μ_a is the apparent viscosity in the porous medium, which is a function of μ_f and φ.

2.2. *Conditions at the interface between a porous medium and a pure fluid*

Based on the axioms of mixture theory given by Truesdell & Toupin (1960), Hou *et al.* (1989) considered the boundary conditions between a fluid and a deformable porous medium using a binary mixture theory and derived a set of boundary conditions based on conservation equations.

$$[\![\varphi\boldsymbol{n}\cdot(\boldsymbol{q}-\dot{\boldsymbol{s}})]\!] = 0, \tag{2.7}$$

$$[\![\boldsymbol{n}\cdot(\boldsymbol{T}^s + \boldsymbol{T}^f - \rho_f\boldsymbol{q}(\boldsymbol{q}-\dot{\boldsymbol{s}}))]\!] = 0, \tag{2.8}$$

where $\boldsymbol{n}$ is the unit vector normal to the surface of discontinuity pointing into the fluid and $[\![\ ]\!]$ denotes the jump from the porous medium into the pure fluid where $\varphi = 1$, $\mu_a = \mu_f$, $q = v$ and $\boldsymbol{T}^s = 0$.

Further conditions at the porous interface are needed to solve the equations. They are the relationship between the tangential velocities at the interface and the distribution of shear stress between the fluid and the solid on the porous side of the interface. We make the following assumptions.

(i) The volume-averaged velocity in the tangential direction is continuous across the porous interface:

$$[\![\varphi \boldsymbol{t}\cdot(\boldsymbol{q}-\dot{\boldsymbol{s}})]\!] = 0, \tag{2.9}$$

where $\boldsymbol{t}$ is the unit vector tangent to the surface.

(ii) The stress distribution between the two phases is proportional to their volume fractions at the interface:

$$\frac{\mu_a \partial q_t/\partial \boldsymbol{n}}{\mu\, \partial s_t/\partial \boldsymbol{n}} = \frac{\varphi}{1-\varphi}, \tag{2.10}$$

where q_t and s_t are the tangential components of the fluid velocity and the solid displacement.

The first assumption is the simplest which leads to the continuity of fluid velocities when $\varphi \to 1$ and the no-slip condition when $\varphi \to 0$. The second assumption dictates the distribution of the surface shear stress between the fluid and the solid at the interface and again is the simplest condition that gives the proper behaviour as φ approaches both 0 and 1. The actual distribution of the shear stress will depend upon the microstructure of the porous material at the surface. Neither of these assumptions can be derived from conservation equations.

3. Geometry

As shown in figure 1, R is the radius of the tube taken to the outer boundary of the porous layer, a is the radius of the sphere, including the thickness of the porous layer, $h(z, \phi)$ is the local clearance between sphere and tube, e is the eccentricity (the distance between the sphere centre and the tube axis). The clearance is defined as $c = R-a$, W is the excess weight of the sphere ($\frac{4}{3}\pi a^3 \Delta\rho\, g$), where $\Delta\rho$ is the density difference between the sphere and the fluid. The cylindrical coordinates are fixed relative to the tube, with their origin at the instantaneous centre of the sphere.

When the radius of the sphere and the radius of the tube are nearly the same, we consider a lubrication zone $-\theta_0 < \theta < \theta_0$ in which there is a thin fluid layer (part of it occupied by the porous layer) where the local clearance h measured parallel to the line from centre of sphere and perpendicular to tube axis can be expressed as

$$h = (R^2 - e^2 \sin^2\phi)^{1/2} + e\cos\phi - (a^2 - z^2)^{1/2}. \tag{3.1}$$

In the gap, the variation of h in the circumferential direction is

$$\frac{\partial h}{\partial \phi} = -e\sin\phi - \frac{e^2 \sin\phi\cos\phi}{(R^2 - e^2\sin^2\phi)^{1/2}} = O(e) \tag{3.2}$$

and its variation in the axial direction is

$$\frac{\partial h}{\partial z} = \frac{z}{(a^2 - z^2)^{1/2}} = O(1). \tag{3.3}$$

The eccentricity of the sphere, e, is bounded by the clearance c. When c is small, the variation of local clearance in the circumferential direction is negligible compared with

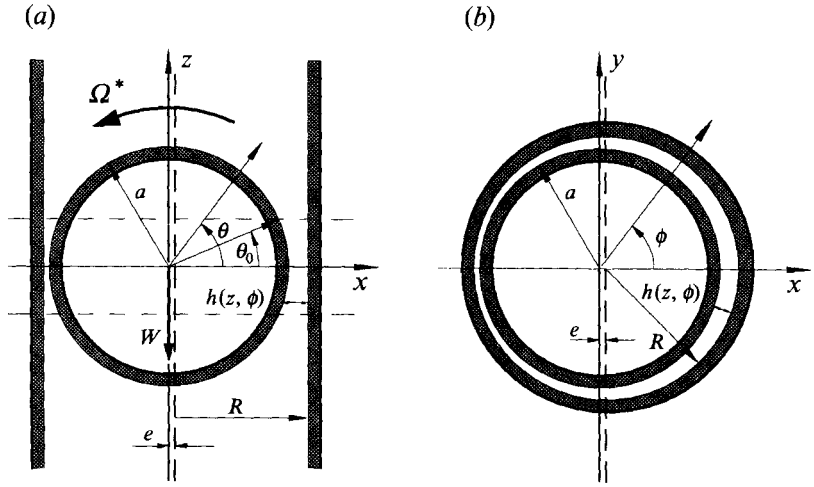

FIGURE 1. Geometry and coordinates of an eccentric sphere of radius a falling in a vertical cylindrical tube of radius R. θ is the angular coordinate in the vertical plane about the axis of rotation of the sphere. ϕ is the angular coordinate about the vertical axis of the sphere defined so that $\phi = 0$ is the point at which the gap is maximum. e is the eccentricity of the centre of the sphere relative to the axis of the tube. $h(z, \phi)$ is the local clearance between the sphere and the tube. W acts in the negative z-direction.

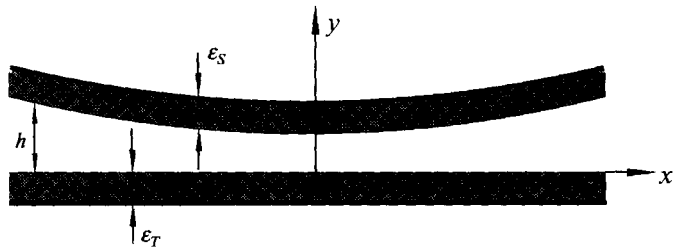

FIGURE 2. Local Cartesian coordinates fixed on the surface of the tube in the lubrication zone. x is in the z-direction, y is the direction pointing to the centre of the sphere, h is the local clearance, ϵ_T is the thickness of the porous layer on the tube and ϵ_S is the thickness of the porous layer on the sphere.

its variation in the axial direction. We therefore assume that, at any given circumferential position, ϕ, the problem can be treated in local two-dimensional Cartesian coordinates fixed at the interface between the fluid and porous layer of the tube (see figure 2). The x-axis is the axial direction of the tube and the y-axis is in the direction pointing instantaneously to the centre of the sphere so that $-\epsilon_T < y < 0$ is the porous layer on the tube, $0 < y < h$ is the pure fluid region and $h < y < h + \epsilon_S$ is the porous layer on the sphere. The porous layers on the surfaces of the tube and sphere can be treated locally as flat plates. Inside the lubrication zone, $-\theta_0 < \theta < \theta_0$, the thickness of the fluid layer is everywhere small compared with the z lengthscale of the zone, and the velocity distribution at any section of the layer is approximately the same as in a uniform layer with the same layer thickness and pressure gradient (Batchelor 1967, pp. 238–240). Because the local clearance h increases very quickly with z outside the lubrication zone, the velocity and pressure gradient there are negligible compared with those inside. The motion of the sphere is thus determined by the flow inside the lubrication zone. We must, of course, check that our results are consistent with our assumption that the circumferential pressure gradients are negligible.

4. Solutions using lubrication theory

In the following analysis, the thicknesses of the porous layers on the tube ϵ_T and on the sphere ϵ_S, the solid displacements in the x-direction s_1 and in the y-direction s_2, the radius of the tube R, the eccentricity e, and the local clearance h are non-dimensionalized by the radius of the sphere, a. Velocities are non-dimensionalized by the descending velocity of the sphere U. The following further non-dimensionalizations are carried out:

$$\text{pressure} \quad p' = aU^{-1}\mu_f^{-1}p,$$

$$\text{drag coefficient} \quad k' = a^2\mu_a^{-1}k,$$

$$\text{excess weight of the sphere} \quad W' = a^{-1}\mu_f^{-1}U^{-1}W,$$

$$\text{rotation velocity of the sphere} \quad \Omega' = aU^{-1}\Omega,$$

where a prime denotes non-dimensional variables. In order to compare the velocities of the sphere for different conditions in the results section, it is convenient to define

$$U^* = UU_\infty^{-1}, \quad \Omega^* = \Omega a U_\infty^{-1},$$

where $U_\infty = W/(6\pi\mu_f a)$ is the Stokes velocity of the sphere in an unbounded fluid. For clarity, the prime is dropped in the equations and results hereafter. The following non-dimensional parameters arise from the non-dimensionalization of the conservation equations in the porous layer:

$$Re_f = \frac{\rho_f U a}{\mu_f}; \quad Re_a = \frac{\rho_f U a}{\mu_a}; \quad \xi = \frac{\mu_a}{\mu_f}; \quad \zeta = \frac{U}{a}\frac{\mu_f}{\mu}; \quad \chi = \frac{\lambda}{\mu}.$$

In the following analysis, the porous layer on the surface of the tube is considered in detail and the results for the porous layer on the sphere are presented. At steady state, in the Cartesian coordinates fixed on the tube, the solid velocities are zero. The governing equations are:

in the pure fluid region

$$\frac{\partial v_1}{\partial x} + \frac{\partial v_2}{\partial y} = 0, \tag{4.1}$$

$$0 = -\frac{\partial p}{\partial x} + \frac{\partial^2 v_1}{\partial x^2} + \frac{\partial^2 v_1}{\partial y^2}, \tag{4.2}$$

$$0 = -\frac{\partial p}{\partial y} + \frac{\partial^2 v_2}{\partial x^2} + \frac{\partial^2 v_2}{\partial y^2}; \tag{4.3}$$

inside the porous layer

$$\frac{\partial q_1}{\partial x} + \frac{\partial q_2}{\partial y} = 0, \tag{4.4}$$

solid phase

$$0 = -(1-\varphi)\zeta\frac{\partial p}{\partial x} + (\chi+2)\frac{\partial^2 s_1}{\partial x^2} + (\chi+1)\frac{\partial^2 s_2}{\partial x\,\partial y} + \frac{\partial^2 s_1}{\partial y^2} + \zeta\xi k q_1, \tag{4.5}$$

$$0 = -(1-\varphi)\zeta\frac{\partial p}{\partial y} + (\chi+2)\frac{\partial^2 s_2}{\partial y^2} + (\chi+1)\frac{\partial^2 s_1}{\partial x\,\partial y} + \frac{\partial^2 s_2}{\partial x^2} + \zeta\xi k q_2, \tag{4.6}$$

fluid phase

$$0 = -\frac{\varphi}{\xi}\frac{\partial p}{\partial x} + \left(\frac{\partial^2 q_1}{\partial x^2} + \frac{\partial^2 q_1}{\partial y^2}\right) - k q_1, \tag{4.7}$$

$$0 = -\frac{\varphi}{\xi}\frac{\partial p}{\partial y} + \left(\frac{\partial^2 q_2}{\partial x^2} + \frac{\partial^2 q_2}{\partial y^2}\right) - k q_2. \tag{4.8}$$

From the jump condition (2.7) we have

$$v_2 = \varphi q_2 \tag{4.9}$$

and from (2.8) we have

$$\frac{\partial v_1}{\partial y}+\frac{\partial v_2}{\partial x} = \frac{1}{\zeta}\left(\frac{\partial s_1}{\partial y}+\frac{\partial s_2}{\partial x}\right)+\xi\left(\frac{\partial q_1}{\partial y}+\frac{\partial q_2}{\partial x}\right), \tag{4.10}$$

$$\frac{\partial v_2}{\partial y} = \frac{\chi}{2\zeta}\left(\frac{\partial s_1}{\partial x}+\frac{\partial s_2}{\partial y}\right)+\frac{1}{\zeta}\frac{\partial s_2}{\partial y}+\xi\frac{\partial q_2}{\partial y}. \tag{4.11}$$

Inside the porous layer on the tube, assuming there are no sudden changes of velocity and pressure in the x-direction, $\partial q_1/\partial x = O(1)$, it can be shown that $q_1 = O(1)$. From the mass conservation equation (4.4), $q_2 = O(\epsilon_T)$ and is negligible compared with q_1. By comparing the order of each term in the momentum equations, it is seen that $\partial p/\partial y$ is negligible compared with $\partial p/\partial x$. To $O(\epsilon_T)$, the fluid momentum equation (4.7) reduces to

$$0 = -\frac{\varphi}{\xi}\frac{\partial p}{\partial x}+\frac{\partial^2 q_1}{\partial y^2}-kq_1. \tag{4.12}$$

The solid momentum equation (4.5) similarly reduces to

$$0 = -(1-\varphi)\,\zeta\frac{\partial p}{\partial x}+\frac{\partial^2 s_1}{\partial y^2}+\zeta\xi k q_1. \tag{4.13}$$

In the pure fluid region inside the lubrication zone, the momentum equation (4.2) simplifies to

$$0 = -\frac{\partial p}{\partial x}+\frac{\partial^2 v_1}{\partial y^2}. \tag{4.14}$$

The boundary conditions are:

$y = -\epsilon_T$ (rigid tube wall)
$$s_1 = 0, \tag{4.15}$$
$$q_1 = 0; \tag{4.16}$$

$y = 0$ (porous interface)
$$\frac{\partial v_1}{\partial y} = \frac{1}{\zeta}\frac{\partial s_1}{\partial y}+\xi\frac{\partial q_1}{\partial y}, \tag{4.17}$$

and the assumptions of matching conditions at the porous interfaces are, from (2.9),

$$v_1 = \varphi q_1 \tag{4.18}$$

and from (2.10)

$$\xi\zeta\frac{\partial q_1}{\partial y}\Big/\frac{\partial s_1}{\partial y} = \frac{\varphi}{1-\varphi}. \tag{4.19}$$

From (4.12) with boundary and matching conditions, the fluid velocity at the interface between the porous layer and the pure fluid can be expressed as

$$v_1 = \frac{\varphi^2}{k^{1/2}\xi}\tanh(k^{1/2}\epsilon_T)\frac{\partial v_1}{\partial y}+\frac{\varphi^2}{k\xi}\frac{1-\cosh(k^{1/2}\epsilon_T)}{\cosh(k^{1/2}\epsilon_T)}\frac{\partial p}{\partial x}. \tag{4.20}$$

From (4.14), $\partial v_1/\partial y$ is of the order of the magnitude of $h\,\partial p/\partial x$. When the lengthscale on which the velocity varies in the porous layer is small compared with the local clearance

$$h \gg \min(\epsilon_T, k^{-1/2}),$$

then $$h \gg \frac{1-\cosh(k^{1/2}\epsilon_T)}{k^{1/2}\sinh(k^{1/2}\epsilon_T)}$$

and the second term on the right-hand side of (4.20) is negligible. The velocity at the porous interface on the tube can be written as

$$v = \kappa_T \frac{\partial v_1}{\partial y}, \tag{4.21}$$

where $$\kappa_T = \frac{\varphi^2}{k^{1/2}\xi}\tanh(k^{1/2}\epsilon_T).$$

This form of boundary condition is similar to that found in other theoretical and experimental work (Beavers & Joseph 1967; Taylor 1971; Richardson 1971; Saffman 1971; Barry *et al.* 1991).

A similar analysis is applied to the porous layer on the surface of the sphere. Considering the rotation and falling velocities of the sphere (positive Ω is the anticlockwise direction (figure 1*a*), positive U is the z-direction (figure 1*b*), the slip velocity at the porous interface on the sphere is

$$y = h: \qquad v_1 = V_s - \kappa_S \frac{\partial v_1}{\partial y}, \tag{4.22}$$

where $$V_s = \Omega\cos\theta\cos\phi - 1$$

is the velocity of the surface of the sphere and

$$\kappa_S = \frac{\varphi_S^2}{k_S^{1/2}\xi_S}\tanh(k_S^{1/2}\epsilon_S)$$

in which the subscript S denotes the parameters of the porous layer on the sphere, κ_S and κ_T are slip parameters. Equations (4.21) and (4.22) are the equivalent slip boundary conditions at the surfaces of the tube and sphere inside the lubrication zone, which represent the hydrodynamic effects of the porous layers on the flow when the lengthscale in the porous layer on which the velocity varies is small compared with the local clearance. These slip boundary conditions are applied in the following derivation of the motion of the sphere and comparison is made between the results with and without slip boundary condition at surfaces of the sphere and the tube. In the local Cartesian coordinates, by solving (4.14) with the boundary conditions (4.21) and (4.22), the velocity at point $(x = \cos\theta, y)$ can be expressed as

$$v_1 = -\tfrac{1}{2}Gy^2 + (V_s + Gh\kappa_S + \tfrac{1}{2}Gh^2)\frac{y+\kappa_T}{h+\kappa_T+\kappa_S}, \tag{4.23}$$

where $G = -\partial p/\partial x$ and $h = h(\theta, \phi)$. The flux per unit circumferential width can be derived by integrating the velocity over the local clearance $h(\theta, \phi)$:

$$Q(\phi) \equiv \int_0^h v_1 \,\mathrm{d}y = -\tfrac{1}{6}Gh^3 + (V_s + Gh\kappa_S + \tfrac{1}{2}Gh^2)\frac{h(h+2\kappa_T)}{2(h+\kappa_T+\kappa_S)}. \tag{4.24}$$

The pressure gradient $G(\theta, \phi)$ can therefore be expressed in terms of the local flux $Q(\phi)$ as

$$G(\theta, \phi) = -\frac{Q}{c_1} + V_s\frac{c_2}{c_1}, \tag{4.25}$$

where $c_1(\theta,\phi) = \frac{1}{6}h^3 - \frac{1}{4}h^2\dfrac{(h+2\kappa_T)(h+2\kappa_S)}{h+\kappa_T+\kappa_S}$, $c_2(\theta,\phi) = \dfrac{h^2+2h\kappa_T}{2(h+\kappa_T+\kappa_S)}$.

The shear stress on the surface of the sphere is

$$\tau(\theta,\phi) = -\mu_f Q\frac{c_2}{c_1} + \mu_f V_s\left(\frac{c_2^2}{c_1} - \frac{1}{h+\kappa_T+\kappa_S}\right). \tag{4.26}$$

The shear force per unit circumferential width on the sphere, $S(\phi)$, can be calculated by integrating the shear stress $\tau(\theta,\phi)$ over the lubrication zone $-\theta_0 < \theta < \theta_0$:

$$S(\phi) = -\mu_f Q\Gamma_1 + \mu_f \Omega\cos\phi\Gamma_2 - \mu_f\Gamma_3, \tag{4.27}$$

where

$$\Gamma_1(\phi) = \int_{-\theta_0}^{\theta_0}\frac{c_2}{c_1}\mathrm{d}\theta, \quad \Gamma_2(\phi) = \int_{-\theta_0}^{\theta_0}\left(\frac{c_2^2}{c_1} - \frac{1}{h+\kappa_T+\kappa_S}\right)\cos\theta\,\mathrm{d}\theta,$$

$$\Gamma_3(\phi) = \int_{-\theta_0}^{\theta_0}\left(\frac{c_2^2}{c_1} - \frac{1}{h+\kappa_T+\kappa_S}\right)\mathrm{d}\theta.$$

The pressure difference can be derived by integrating $-G$ over the lubrication zone:

$$\Delta p = Q\Gamma_4 - \Omega\cos\phi\Gamma_5 + \Gamma_1, \tag{4.28}$$

where $\Gamma_4(\phi) = \int_{-\theta_0}^{\theta_0}\frac{1}{c_1}\mathrm{d}\theta$, $\Gamma_5(\phi) = \int_{-\theta_0}^{\theta_0}\frac{c_2}{c_1}\cos\theta\,\mathrm{d}\theta$.

In the lubrication limit, at steady state, the excess weight of the sphere is balanced by the force due to the pressure difference (Christopherson & Dowson 1959; Chester 1984):

$$-\Delta p\,\pi = W. \tag{4.29}$$

From (4.28)

$$Q = \frac{1}{\Gamma_4}\left(-\frac{W}{\pi} + \Omega\cos\phi\,\Gamma_5 - \Gamma_1\right). \tag{4.30}$$

The total torque on the sphere due to the shear stress can be derived by integrating the local shear force $S(\phi)$ over the sphere:

$$T \equiv \int_0^{2\pi} S(\phi)\cos\phi\,\mathrm{d}\phi = \mu_f\left(\frac{W}{\pi}\Lambda_1 + \Omega\Lambda_2 + \Lambda_3\right), \tag{4.31}$$

where

$$\Lambda_1 = \int_0^{2\pi}\frac{\Gamma_1}{\Gamma_4}\cos\phi\,\mathrm{d}\phi, \quad \Lambda_2 = \int_0^{2\pi}\left(\Gamma_2 - \frac{\Gamma_1\Gamma_5}{\Gamma_4}\right)\cos^2\phi\,\mathrm{d}\phi, \quad \Lambda_3 = \int_0^{2\pi}\left(\frac{\Gamma_1^2}{\Gamma_4} - \Gamma_3\right)\cos\phi\,\mathrm{d}\phi.$$

At steady state, the total torque on the sphere is zero, so from (4.31)

$$\Omega = -\frac{\Lambda_1 W + \pi\Lambda_3}{\pi\Lambda_2}. \tag{4.32}$$

The total flux can be derived by integrating the local flux $Q(\phi)$ over the sphere ($0 \leqslant \phi < 2\pi$):

$$\pi R^2 = \int_0^{2\pi} Q\,\mathrm{d}\phi = \frac{W}{\pi}\Lambda_4 + \Lambda_5, \tag{4.33}$$

where $\Lambda_4 = -\int_0^{2\pi} \frac{1+\cos\phi\,\Gamma_5\Lambda_1/\Lambda_2}{\Gamma_4}\mathrm{d}\phi$, $\Lambda_5 = -\int_0^{2\pi} \frac{\Gamma_1+\cos\phi\,\Gamma_5\Lambda_3/\Lambda_2}{\Gamma_4}\mathrm{d}\phi$.

The descending velocity of the sphere relative to the Stokes velocity U_∞ is

$$U^* = \frac{6\Lambda_4}{\pi R^2 - \Lambda_5} \tag{4.34}$$

and the rotation of the sphere relative to U_∞/a is

$$\Omega^* = -\frac{6\Lambda_1 + \Lambda_3 U^*}{\Lambda_2}. \tag{4.35}$$

The integrals in the above equations were evaluated numerically using the trapezoidal rule and the results are presented in the following section.

5. Results

The solutions in the previous section presume that the clearance between the sphere and tube is small compared with the radius of the sphere, so that lubrication theory is applicable in the region around the point of minimum clearance $-\theta_0 < \theta < \theta_0$. The axial pressure gradient and velocity outside this zone are negligible compared with those inside, so it is the flow in this region that determines the movement of the sphere. To show the validity of this assumption, velocities of the sphere are plotted as functions of θ_0 in figure 3 with clearances $c = 0.1$, 0.05 and 0.025, eccentricity $e/c = 0.5$ and assuming no-slip boundary conditions. It is seen that when θ_0 is small, U^* and Ω^* are very sensitive to the choice of θ_0. However, when θ_0 is larger than a certain value, the velocities are almost independent of θ_0. For a smaller clearance, $c = 0.025$, the width of the sensitive zone is seen to be smaller than when $c = 0.1$. By comparing figures 3(*a*) and 3(*b*), it is also seen that Ω^* is more sensitive to θ_0 than U^*. In all of the following results, we have used $\theta_0 = 2\pi/9$ ($\approx 40°$).

It can be seen from symmetry arguments that the use of slip boundary conditions does not alter the result that there is no sideways movement of the sphere in the absence of inertial terms (Christopherson & Dowson 1959; Bungay & Brenner 1973).

Figure 4 shows the variation of U^* and Ω^* with the radius of the tube R, with the eccentricity $e/c = 0.5$ and the no-slip boundary conditions. When the clearance approaches zero, both U^* and Ω^* approach zero. The velocities increase as the clearance gets larger and the increase becomes faster at larger clearance. Ω^* is seen to be much larger than U^*. Similar results are seen when the slip boundary conditions are applied.

For a given R, the velocity and rotation are functions of e and the slip parameters κ_T and κ_S. We consider thin porous layers for the glycocalyx. Based on estimations that ϵ_T and ϵ_S are about 0.02, $\varphi \approx 0.7$ and $\xi \approx 1$ (Brinkman 1947; Lundgren 1972; Kolodziej 1988), we take the slip parameters κ_T and κ_S to be 0.01 in the calculations when slip boundary conditions are applied. Figure 5(*a*) shows the variation of U^* with the eccentricity e for four different boundary conditions: (i) no-slip boundary conditions at the surfaces of both the tube and the sphere ($\kappa_T = 0, \kappa_S = 0$), (ii) slip at the tube wall but no-slip at the sphere surface ($\kappa_T = 0.01$, $\kappa_S = 0$), (iii) no-slip at the tube wall but slip at the sphere surface ($\kappa_T = 0$, $\kappa_S = 0.01$) and (iv) slip at both surfaces ($\kappa_T = 0.01$, $\kappa_S = 0.01$). It is seen that the velocity of the sphere increases as it moves away from the centre of the tube. The descending velocity of the sphere increases when

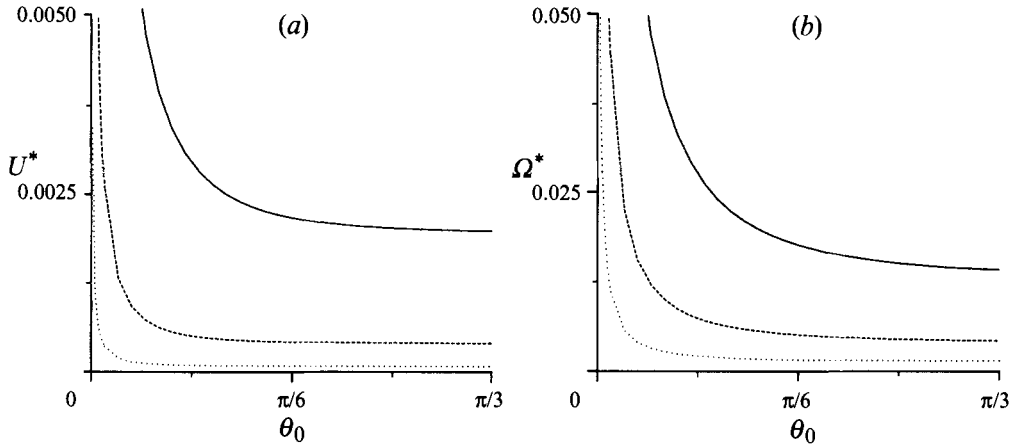

FIGURE 3. Sensitivity of velocities of the sphere to the width of the lubrication zone θ_0. $e/c = 0.5$, $\kappa_T = 0$, $\kappa_S = 0$. ——, $c = 0.1$; – – – – –, $c = 0.05$; ....., $c = 0.025$. (*a*) Descending velocity of the sphere U^*, (*b*) rotation of the sphere Ω^*.

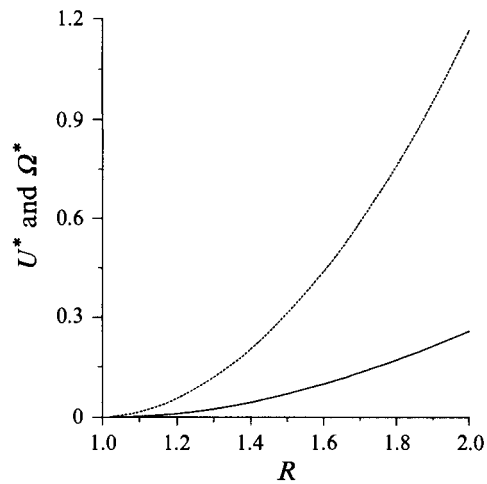

FIGURE 4. Variation of the velocities of the sphere, U^* and Ω^*, with the radius of the tube, R. $e/c = 0.5$, $\kappa_T = 0$, $\kappa_S = 0$. ——, U^*; ....., Ω^*.

slip boundary conditions are applied. By comparing the two middle curves ($\kappa_T = 0.01$, $\kappa_S = 0$) and ($\kappa_T = 0, \kappa_S = 0.01$), the slip parameter on the sphere surface has a slightly larger influence on U^* than that on the tube wall. Figure 5(*b*) shows the variation of Ω^* with e, for the same conditions. Ω^* increases from zero, when the sphere is on the axis of the tube, to a maximum value before decreasing as e approaches the gap width. Note that the direction of the rotation is opposite to that when the sphere is rolling on the nearer tube wall. The decrease of the rotation after e exceeds a certain value is caused by the rapid increase of the shear stress on the narrower side of the gap where the local clearance is very small. When slip boundary conditions are applied, the rotation of the sphere increases. To see the overall effects of the slip boundary conditions on U^* and Ω^*, figure 5(*c*) shows the variation of Ω^*/U^* with e. Ω^* increases much faster than U^* with e and overtakes U^* at a small eccentricity. It is seen that although the slip boundary conditions increase both U^* and Ω^*, the ratio Ω^*/U^* decreases.

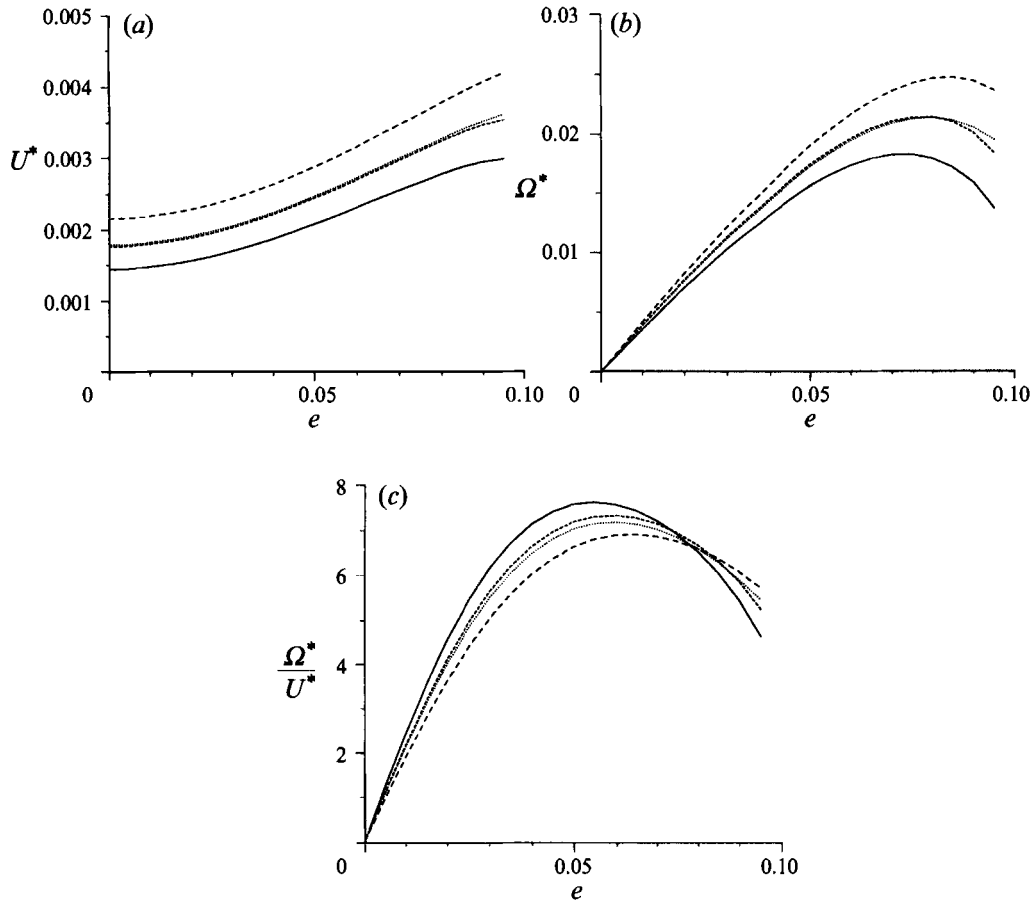

FIGURE 5. Variations of the velociites of the sphere with e for different boundary conditions. $R = 1.1$. ——, $\kappa_T = 0$, $\kappa_S = 0$; – – – –, $\kappa_T = 0.01$, $\kappa_S = 0$; ....., $\kappa_T = 0$, $\kappa_S = 0.01$; ——— —, $\kappa_T = 0.01$, $\kappa_S = 0.01$. (*a*) Descending velocity of the sphere U^*, (*b*) rotation of the sphere Ω^*, (*c*) Ω^*/U^*.

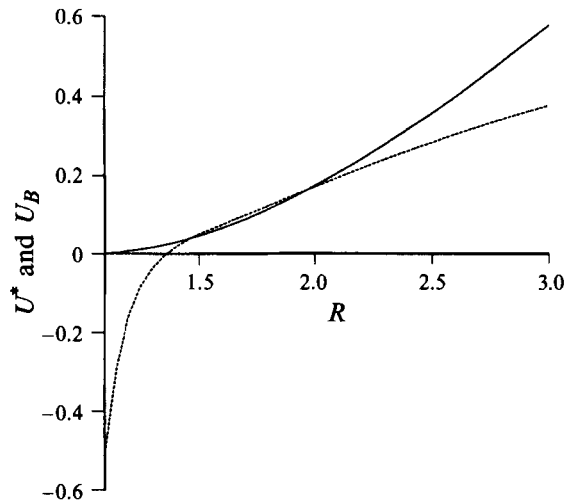

FIGURE 6. Comparison between U^* from lubrication theory (——) and U_B from Bohlin's approximation (.....) when $e = 0$, $\kappa_T = 0$, $\kappa_S = 0$.

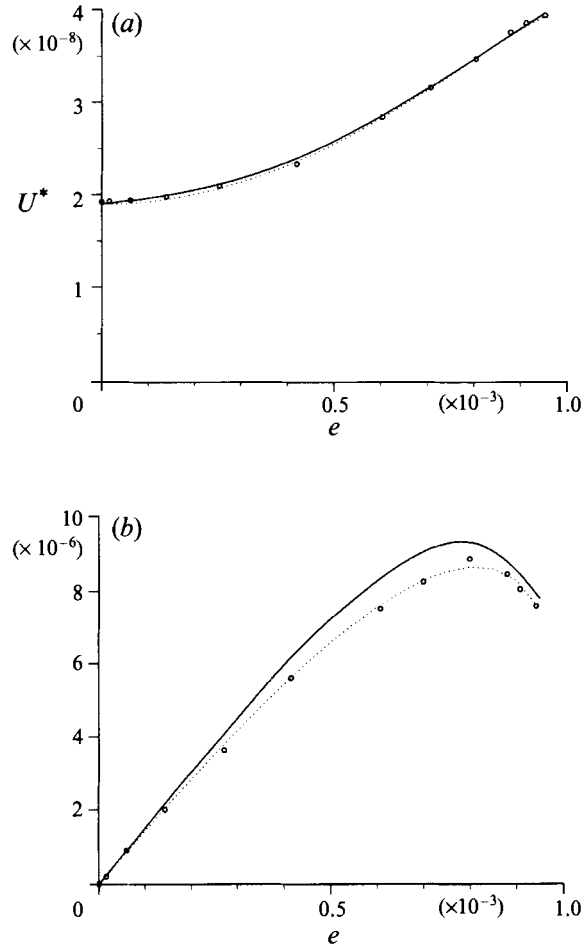

FIGURE 7. Comparison of U^* and Ω^* with Bungay & Brenner's results (5.2) (.....) and results taken from Christopherson & Dowson (○) at different eccentricity when $c = 0.001$, $\kappa_T = 0$, $\kappa_S = 0$. (*a*) U^*, (*b*) Ω^*.

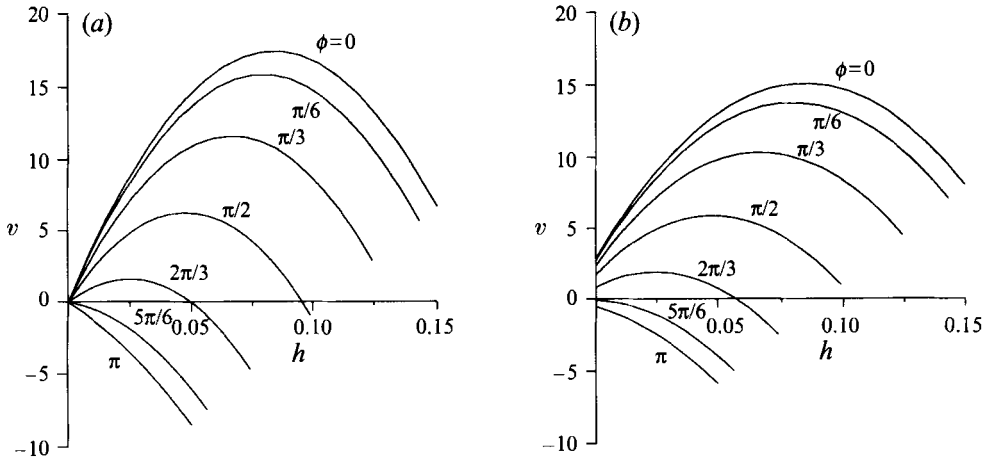

FIGURE 8. Fluid velocity profiles in the $\theta = 0$ plane for specified ϕ. $R = 1.1$ and $e = 0.05$. (*a*) $\kappa_T = 0$, $\kappa_S = 0$, (*b*) $\kappa_T = 0.01$, $\kappa_S = 0.01$.

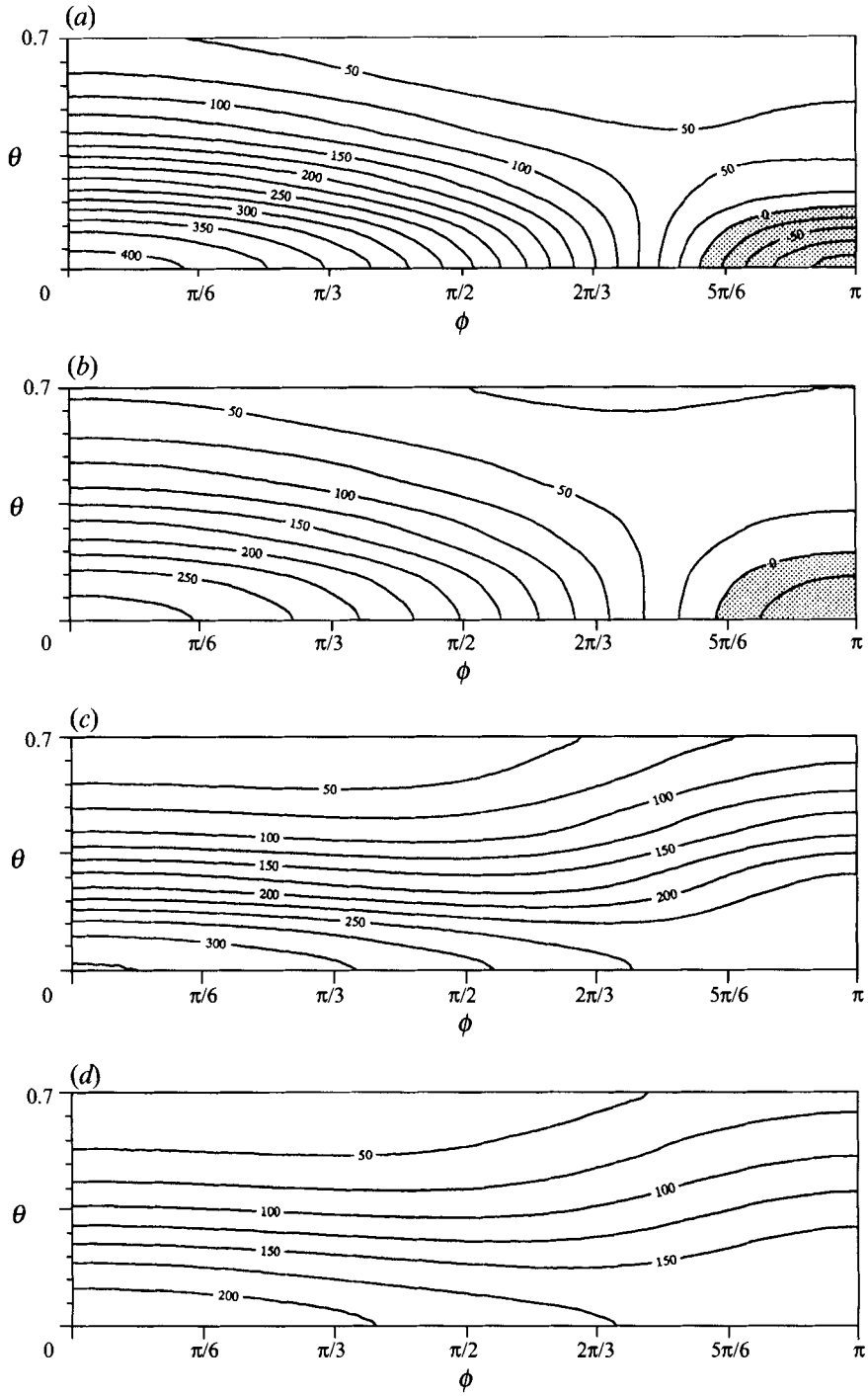

FIGURE 9. Shear stress contours on the surfaces of the tube and the sphere with different boundary conditions. $R = 1.1$ and $e = 0.05$. For the no-slip conditions, $U^* = 0.0021$ and $\Omega^* = 0.0155$ and for the slip conditions, $U^* = 0.0029$ and $\Omega^* = 0.0189$. (*a*) On the surface of the tube, $\kappa_T = 0$, $\kappa_S = 0$; (*b*) on the surface of the tube, $\kappa_T = 0.01$, $\kappa_S = 0.01$; (*c*) on the surface of the sphere, $\kappa_T = 0$, $\kappa_S = 0$; (*d*) on the surface of the sphere, $\kappa_T = 0.01$, $\kappa_S = 0.01$.

Bohlin (1960) studied the problem of a sphere's motion on the axis of a tube using a reflection method and gave the following formula of the velocity of the sphere relative to the Stokes velocity:

$$U_B = 1 - \frac{2.10443}{R} + \frac{2.08877}{R^3} - \frac{0.94813}{R^5} - \frac{1.372}{R^6} + \frac{3.87}{R^8} - \frac{4.19}{R^{10}} + \ldots. \tag{5.1}$$

It is an approximate solution, which gives good results when the radius of the tube is large. Figure 6 compares U_B with U^* applying no-slip boundary conditions and zero eccentricity. When the radius of the tube is small (R approaches 1), Bohlin's approximation is not valid. The lubrication theory, on the other hand, gives increasingly good accuracy. When the gap is big, the lubrication solution is no longer valid and deviates from Bohlin's results.

Bungay & Brenner (1973) analysed the sedimentation of a closely fitting sphere in a fluid-filled tube using a singular perturbation method. In our notation, the results obtained (their equations 8.4 and 8.5) are

$$U^* = \frac{4\sqrt{2}}{3\pi}\left(\frac{1}{\eta_0} + \frac{(e/c)^2}{2\eta_3}\right)c^{5/2} + O(c^3), \quad \Omega^* = \frac{\sqrt{2e/c}}{\pi\eta_3}c^{3/2} + O(c^2), \tag{5.2}$$

where $$\eta_0 = \frac{2\pi}{\int_{-\pi}^{\pi}(1-(e/c)\cos\phi)^{5/2}\,\mathrm{d}\phi}, \quad \eta_3 = \frac{1}{\pi}\int_{-\pi}^{\pi}\frac{\cos^2\phi}{(1-(e/c)\cos\phi)^{1/2}}\,\mathrm{d}\phi.$$

Figure 7 shows a comparison of our calculations with those of Christopherson & Dowson (1959) and Bungay & Brenner (1973) for the velocities as a function of e when the clearance $c = 0.001$. Good agreement between all of the theories is seen for U^* (figure 7*a*), but our result for Ω^* (figure 7*b*) differs slightly. This difference decreases for smaller values of c. By comparing this figure with figure 5, it can be seen that both U^* and Ω^* decrease with decreasing c. The ratio Ω^*/U^*, however, increases.

Figure 8 shows the velocity profiles along the equator of the sphere, $\theta = 0$, at different values of the circumferential angle, ϕ, for $R = 1.1$ and $e = 0.05$. The fluid velocities for the no-slip boundary conditions are shown in figure 8(*a*) and those of the slip boundary conditions ($\kappa_T = 0.01$, $\kappa_S = 0.01$) in figure 8(*b*). Since the sphere has an eccentricity, the local clearance, h, varies from 0.15 when $\phi = 0$ to 0.05 when $\phi = \pi$. The velocities change from positive at the maximum clearance to negative at the minimum clearance. With the slip boundary conditions, the velocity profiles are flatter with a reduced maximum and reduced gradients at the walls of the tube and sphere.

Figure 9 shows the shear stress distribution inside the lubrication zone on the surface of both the tube and the sphere with no-slip and slip boundary conditions for $R = 1.1$ and $e = 0.05$. $U^* = 0.0021$ and $\Omega^* = 0.0155$ with no-slip boundary conditions, and $U^* = 0.0029$ and $\Omega^* = 0.0189$ with slip boundary conditions. Because of the symmetries, only one quarter of the surfaces are plotted. On the tube wall, the maximum shear stress occurs at $\theta = 0$ where the local clearance is the least and decreases quickly as θ increases towards the edge of the lubrication zone where the shear stresses are about 1/10 of their values at the central area. The shear stress on the tube wall is positive at the maximum clearance, decreasing as the gap decreases to a negative minimum value at $\phi = \pi$. On the surface of the sphere, however, the shear stress is always positive. By comparing the slip and no-slip conditions, it is seen that the slip boundary conditions ($\kappa_T = 0.01, \kappa_S = 0.01$) generally reduce the shear stresses on both surfaces.

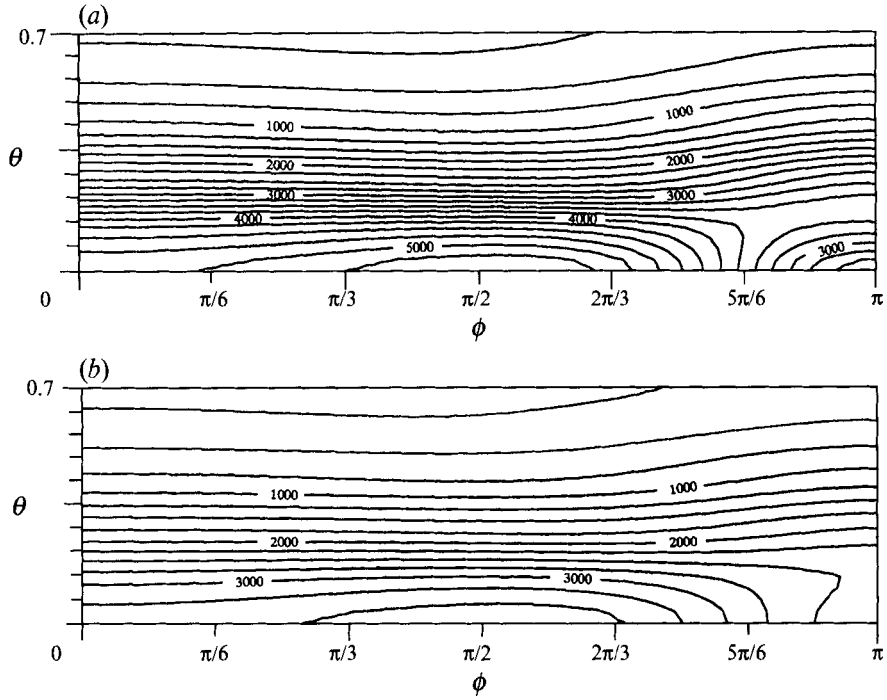

FIGURE 10. Pressure gradient, $G = -\partial p/\partial x$, contours in the lubrication zone. $R = 1.1$ and $e = 0.05$. For the no-slip condition, $U^* = 0.0021$ and $\Omega^* = 0.0155$ and for the slip conditions, $U^* = 0.0029$ and $\Omega^* = 0.0189$. (*a*) $\kappa_T = 0$, $\kappa_S = 0$; (*b*) $\kappa_T = 0.01$, $\kappa_S = 0.01$.

Figure 10 shows the distribution of the pressure gradient, G, inside the lubrication zone for the same conditions as figure 9. G is largest at the minimum clearance, $\theta = 0$, and decreases very quickly as θ increases, so that at the edge of the lubrication zone, G is relatively small which is consistent with the assumption that the pressure variation outside the lubrication zone is negligible. Along the equator of the sphere, $\theta = 0$, G increases slightly, with ϕ reaching a maximum value at $\pi/2$, and then decreases relatively quickly. This is due to the rotation of the eccentric sphere, which influences the flow pattern at different circumferential positions. The influence of slip boundary conditions ($\kappa_T = 0.01$, $\kappa_S = 0.01$) on G is shown in figure 10(*b*). The pressure gradient in the lubrication zone is greatly reduced when slip boundary conditions are applied. The parallelness of the pressure gradient contours in the circumferential direction shows consistency with our assumption that the circumferential pressure gradient is negligible compared to the axial pressure gradient.

6. Discussion

Analysis of a deformable porous layer using binary mixture theory shows that, when the lengthscale on which the velocity varies in the porous layer is small compared with the local clearance between the sphere and the tube, the effect of the porous layer can be represented by a simple slip condition applied at the interface between the porous layer and the pure fluid. This can result from two different conditions: the porous layer being thin, $\epsilon \ll h$, or the drag coefficient being large so that $k^{-1/2} \ll h$ and the fluid movement in the porous layer is confined to a thin region near the interface.

Two assumptions at the interface between the porous layer and the fluid are made.

The first assumption, (2.9), is that the velocity tangential to the surface is continuous across the interface. If a discontinuity is allowed and the volume-averaged velocity in the porous medium is proportional to the fluid velocity then the boundary conditions (4.21) and (4.22) are unchanged but the slip parameters, κ_T and κ_S, are modified by the constant of proportionality. The second assumption, (2.10), concerns the distribution of the shear stress within the porous layer. Assuming a different distribution again leads to the same form of boundary conditions, (4.21) and (4.22), but with modifications to the slip parameters. Both (2.9) and (2.10) are the simplest assumptions that lead to the proper conditions when the fluid volume fraction approaches either 1 or 0.

Lubrication theory was used to study the motion of a sphere in a tube when the clearance between the sphere and the tube is small compared with the radius of the sphere. The results when the sphere is in the centre of the tube and the no-slip boundary conditions are used complement previous calculations using the method of reflections (Bohlin 1960), coinciding at moderate values of the clearance and providing a reasonable result when the clearance is small. The calculations when the sphere is placed off the axis of the tube can only be compared to the results by Christopherson & Dowson (1959) who used a minimum energy argument to calculate the stable position of a falling sphere in a narrow tube. Good agreement is seen when the clearance is small. The rotation of the sphere is in the opposite sense to that it would have if it were rolling down the nearest wall as shown by Christopherson & Dowson (1959) and Bungay & Brenner (1973). This rotation has the effect of facilitating flow through the region with the largest gap and hence the lowest resistance. As the eccentricity increases, the descending velocity of the sphere increases relatively slowly until it reaches a maximum just before the sphere touches the wall of the tube. The rotation of the sphere also increases as the eccentricity increases until it reaches a maximum some time before contact is made. Except for a very small region near the centre of the tube, the ratio of the rotational velocity to the descending velocity is greater than one. The ratio of the two velocities increases with decreasing clearance.

As would be expected, the use of slip conditions on the walls of the sphere and the tube to model the effects of porous layers increases both the falling and rotational velocities. Over the range of conditions studied, the results for slip conditions on the sphere alone were very slightly larger than the results for slip conditions on the tube alone and the effects were approximately additive when slip conditions were applied at both surfaces. With slip boundary conditions, the pressure gradient and the shear stresses on both surfaces decrease significantly. The magnitude of the effect depends, of course, upon the slip parameters which are used. Lack of information about the composition and properties of the glycocalyx make it difficult to calculate a realistic slip parameter for physiological flows. The properties used to calculate the slip parameters used in this study are not unreasonable but they should be taken as estimates, not definitive descriptions of the glycocalyx on either red blood cells or the endothelial cells lining blood vessels. The glycocalyx is highly charged and charge effects will affect its deformability and will also influence the flow by creating streaming potentials which are not considered in this paper. The linear effects of the fixed charge of the glycocalyx on its mechanical properties, i.e. its elasticity and permeability, are, however, included in the theory through their effect on the Lamé coefficients and the permeability. In any case, this study does indicate that the presence of a glycocalyx-like layer can have a significant influence on the motion of a particle moving through a narrow tube. One case which would be interesting to study is when the gap is so small that the porous layers on the sphere and the tube wall touch each other. In this case,

solid contact forces must be considered and the motion of the sphere could be quite different from that predicted by lubrication theory. The calculation of motion of a sphere in a cylindrical tube with no porous layers itself would have some applications in the studies of transport of particles through a pore, which is of interest in many physiological contexts (e.g. Hill & Hill 1987).

We would like to thank Dr C. G. Phillips for helpful discussions on the slip boundary condition for the porous layer.

REFERENCES

BARRY, S. I., PARKER, K. H. & ALDIS, G. K. 1991 Fluid-flow over a thin deformable porous layer. *Z. Angew. Math. Phys.* **42**, 633–648.

BATCHELOR, G. K. 1967 *An Introduction to Fluid Dynamics*. Cambridge University Press. Section 4.9, pp. 238–240.

BEAVERS, G. S. & JOSEPH, D. D. 1967 Boundary condition at a naturally permeable wall. *J. Fluid Mech.* **30**, 197–207.

BOHLIN, T. 1960 On the drag on a rigid sphere moving in a viscous liquid inside a cylindrical tube. *Trans. R. Inst. Technol. Stockholm* **155**, 64.

BOWEN, R. M. 1980 Incompressible porous media models by the theory of mixture. *Intl J. Engng Sci.* **18**, 1129–1148.

BRENNER, H. & HAPPEL, J. 1958 Slow viscous flow past a sphere in a cylindrical tube. *J. Fluid Mech.* **4**, 195–213.

BRINKMAN, H. K. 1947 A calculation of the viscous force exerted by a flowing fluid on a dense swarm of particles. *Appl. Sci. Res.* A1, 27–34.

BUNGAY, P. M. & BRENNER, H. 1973 The motion of a closely-fitting sphere in a fluid-filled tube. *Intl J. Multiphase Flow* **1**, 25–56.

CARO, C. G. 1982 Arterial fluid-mechanics and atherogenesis. *Clinical Hemorheol.* **2**, 131–136.

CHESTER, W. 1984 The motion of a sphere down a liquid-filled tube. *Proc. R. Soc. Lond.* A **396**, 205–215.

CHRISTOPHERSON, D. G. & DOWSON, D. 1959 An example of minimum energy dissipation in viscous flow. *Proc. R. Soc. Lond.* A **251**, 550–564.

COKELET, G. R., MERRILL, E. W., GILLILAND, E. R., SHIN, H., BRITTEN, A. & WELLS, R. E. 1963 The rheology of human blood measurement near and at zero shear rate. *Trans. Soc. Rheol.* **7**, 303–317.

CURRY, F. E. 1984 Mechanics and thermodynamics of transcapillary exchange. In *Handbook of Physiology, Section 2: The Cardiovascular System. Vol. 4, Microcirculation*, part 1, pp. 309–374. American Physiological Society.

FUNG, Y. C. & LIU, S. Q. 1993 Elementary mechanics of the endothelium of blood vessels. *J. Biomech. Engng* **115**, 1–12.

HALDENBY, K. A., CHAPPELL, D. C., WINLOVE, C. P., PARKER, K. H. & FIRTH, J. A. 1994 Focal and regional variations in the composition of the glycocalyx of large vessel endothelium. *J. Vasc. Biol.* **31**, 2–9.

HILL, A. E. & HILL, B. S. 1987 Steady-state analysis of ion fluxes in necturus gallbladder epithelial-cells. *J. Physiol. Lond.* **382**, 15–34.

HOU, J. S., HOLMES, M. H., LAI, W. M. & MOW, V. C. 1989 Boundary conditions at the cartilage-synovial fluid interface for joint lubrication and theoretical verifications. *J. Biomech. Engng* **111**, 78–87.

KENYON, D. E. 1976 The theory of an incompressible solid-fluid mixture. *Arch. Rat. Mech. Anal.* **62**, 131–147.

KENYON, D. E. 1979 A mathematical model of water flux through aortic tissue. *Bull. Math. Biol.* **41**, 79–90.

KOLODZIEJ, J. A. 1988 Influence of the porosity of a porous-medium on the effective viscosity in Brinkman filtration equation. *Acta Mechanica* **75**, 241–254.

LAI, W. M., HOU, J. S. & MOW, V. C. 1991 A triphasic theory for the swelling and deformation behaviours of articular cartilage. *J. Biomech. Engng* **113**, 245–258.

LANIR, Y., DIKSTEIN, S., HARTZSHTARK, A. & MANNY, V. 1990 In vivo indentation of human skin. *J. Biomech. Engng* **112**, 63–69.

LUNDGREN, T. S. 1972 Slow flow through stationary random beds and suspensions of spheres. *J. Fluid Mech.* **51**, 273–299.

MERRILL, E. W., BENIS, A. M., GILLILAND, E. R., SHERWOOD, T. K. & SALZMAN, E. W. 1965 Pressure-flow relations of human blood in hollow fibres at low flow rates. *J. Appl. Physiol.* **20**, 954–967.

MOW, V. C., KWAN, M. K., LAI, W. M. & HOLMES, M. H. 1985 A finite deformation theory for nonlinearly permeable soft hydrated biological tissues. In *Frontiers in Biomechanics* (ed. G. Schmid-Schoenbein, S. L.-Y. Woo & B. W. Zweifach), pp. 153–179. Springer.

NEREM, R. M. & GIRARD, P. R. 1990 Hemodynamic influences on vascular endothelial biology. *Toxic. Pathol.* **18**, 572–582.

RICHARDSON, S. 1971 A model for the boundary condition of a porous material. Part 2. *J. Fluid Mech.* **49**, 327–336.

SAFFMAN, P. G. 1971 On the boundary condition at the surface of a porous medium. *Stud. Appl. Maths* **1**, 93–101.

SECOMBE, T. W., SKALAK, R., ÖZKAYA, N. & GROSS, J. F. 1986 Flow of axisymmetric red blood cells in narrow capillaries. *J. Fluid Mech.* **163**, 405–423.

SILBERBERG, A. 1991 Polyelectrolytes at the endothelial cell surface. *Biophys. Chem.* **41**, 9–13.

TAYLOR, G. I. 1971 A model for the boundary condition of a porous material. *J. Fluid Mech.* **49**, 319–326.

TRUESDELL, C. & TOUPIN, R. A. 1960 *The Classical Field Theories*. Handbuch der Physik III/1, Springer.

WANG, H. & SKALAK, R. 1969 Viscous flow in a cylindrical tube containing a line of spherical particles. *J. Fluid Mech.* **38**, 75–96.